Highly Conserved Protective Epitopes on Influenza B Viruses

Cyrille Dreyfus *et al.*

Science **337**, 1343 (2012);
DOI: 10.1126/science.1222908

Science (print ISSN 0036-8075; online ISSN 1095-9203) is published weekly, except the last week in December, by the American Association for the Advancement of Science, 1200 New York Avenue NW, Washington, DC 20005.

could be further stabilized by synaptotagmin and complexin (*12*, *18*, *20*) (Fig. 4).

The elegant molecular logic of the SNARE complex thus revealed perfectly fits to precise regulation of neurotransmitter release (*3*), with slow intrinsic assembly of NTD to allow control of vesicle priming by regulatory factors that accelerate NTD assembly, thereby creating the readily releasable pool of neurotransmitters (*11*); an intrinsic pause near the ionic layer stabilized by the repulsion between membranes being forced to fuse to enable clamping by complexin at this stage of zippering (*17*); and unobstructed, fast zippering of CTD and LD to open the fusion pore once the clamp is removed, enabling neurotransmitters to be rapidly released. The pore then expands as the transmembrane domains of VAMP2 and syntaxin dimerize (*32*).

References and Notes

1. T. Söllner *et al.*, *Nature* **362**, 318 (1993).
2. T. Weber *et al.*, *Cell* **92**, 759 (1998).
3. T. C. Südhof, J. E. Rothman, *Science* **323**, 474 (2009).
4. R. B. Sutton, D. Fasshauer, R. Jahn, A. T. Brunger, *Nature* **395**, 347 (1998).
5. P. I. Hanson, R. Roth, H. Morisaki, R. Jahn, J. E. Heuser, *Cell* **90**, 523 (1997).
6. F. S. Cohen, G. B. Melikyan, *J. Membr. Biol.* **199**, 1 (2004).
7. T. Xu *et al.*, *Cell* **99**, 713 (1999).
8. S. Y. Hua, M. P. Charlton, *Nat. Neurosci.* **2**, 1078 (1999).
9. T. J. Melia *et al.*, *J. Cell Biol.* **158**, 929 (2002).
10. A. V. Pobbati, A. Stein, D. Fasshauer, *Science* **313**, 673 (2006).
11. A. M. Walter, K. Wiederhold, D. Bruns, D. Fasshauer, J. B. Sørensen, *J. Cell Biol.* **188**, 401 (2010).
12. M. Kyoung *et al.*, *Proc. Natl. Acad. Sci. U.S.A.* **108**, E304 (2011).
13. C. Cecconi, E. A. Shank, C. Bustamante, S. Marqusee, *Science* **309**, 2057 (2005).
14. Materials and methods in the supplementary materials.
15. K. Weninger, M. E. Bowen, S. Chu, A. T. Brunger, *Proc. Natl. Acad. Sci. U.S.A.* **100**, 14800 (2003).
16. A. Stein, G. Weber, M. C. Wahl, R. Jahn, *Nature* **460**, 525 (2009).
17. Y. Gao, G. Sirinakis, Y. L. Zhang, *J. Am. Chem. Soc.* **133**, 12749 (2011).
18. D. Kümmel *et al.*, *Nat. Struct. Mol. Biol.* **18**, 927 (2011).
19. D. Fasshauer, R. B. Sutton, A. T. Brunger, R. Jahn, *Proc. Natl. Acad. Sci. U.S.A.* **95**, 15781 (1998).
20. F. Li *et al.*, *Nat. Struct. Mol. Biol.* **18**, 941 (2011).
21. Z. Q. Xi, Y. Gao, G. Sirinakis, H. L. Guo, Y. L. Zhang, *Proc. Natl. Acad. Sci. U.S.A.* **109**, 5711 (2012).
22. M. T. Woodside *et al.*, *Science* **314**, 1001 (2006).
23. B. L. Sabatini, W. G. Regehr, *Nature* **384**, 170 (1996).
24. J. Kubelka, J. Hofrichter, W. A. Eaton, *Curr. Opin. Struct. Biol.* **14**, 76 (2004).
25. J. F. Ellena *et al.*, *Proc. Natl. Acad. Sci. U.S.A.* **106**, 20306 (2009).
26. Y. Xu, L. J. Su, J. Rizo, *Biochemistry* **49**, 1568 (2010).
27. E. Karatekin *et al.*, *Proc. Natl. Acad. Sci. U.S.A.* **107**, 3517 (2010).
28. K. Wiederhold, D. Fasshauer, *J. Biol. Chem.* **284**, 13143 (2009).
29. K. Weninger, M. E. Bowen, U. B. Choi, S. Chu, A. T. Brunger, *Structure* **16**, 308 (2008).
30. W. Liu, V. Montana, V. Parpura, U. Mohideen, *J. Nanoneurosci.* **1**, 120 (2009).
31. F. Li *et al.*, *Nat. Struct. Mol. Biol.* **14**, 890 (2007).
32. L. Shi *et al.*, *Science* **335**, 1355 (2012).

Acknowledgments: We thank H. Ji and W. Xu for technical assistance and F. Pincet, T. Melia, and E. Karatekin for valuable discussion. This work is supported by NIH grants GM093341 to Y.Z. and DK027044 to J.E.R. Y.Z. designed the experiments; Y.G., S.Z., G.G., Z.X., L.M., and G.S. performed the experiments; Y.Z. and Y.G. analyzed the data; and Y.Z. and J.E.R. wrote the paper. The data and Matlab codes are in the paper and the supplementary materials.

Supplementary Materials

www.sciencemag.org/cgi/content/full/science.1224492/DC1
Materials and Methods
Figs. S1 to S13
Table S1
References (*33*–*68*)

9 May 2012; accepted 7 August 2012
Published online 16 August 2012;
10.1126/science.1224492

Highly Conserved Protective Epitopes on Influenza B Viruses

Cyrille Dreyfus,[1]* Nick S. Laursen,[1,2]* Ted Kwaks,[3] David Zuijdgeest,[3] Reza Khayat,[1] Damian C. Ekiert,[1]† Jeong Hyun Lee,[1] Zoltan Metlagel,[1]‡ Miriam V. Bujny,[3] Mandy Jongeneelen,[3] Remko van der Vlugt,[3] Mohammed Lamrani,[3] Hans J. W. M. Korse,[3] Eric Geelen,[3] Özcan Sahin,[3] Martijn Sieuwerts,[3] Just P. J. Brakenhoff,[3] Ronald Vogels,[3] Olive T. W. Li,[4] Leo L. M. Poon,[4] Malik Peiris,[4] Wouter Koudstaal,[3] Andrew B. Ward,[1] Ian A. Wilson,[1,5]§ Jaap Goudsmit,[3]§ Robert H. E. Friesen[3]

Identification of broadly neutralizing antibodies against influenza A viruses has raised hopes for the development of monoclonal antibody–based immunotherapy and "universal" vaccines for influenza. However, a substantial part of the annual flu burden is caused by two cocirculating, antigenically distinct lineages of influenza B viruses. Here, we report human monoclonal antibodies, CR8033, CR8071, and CR9114, that protect mice against lethal challenge from both lineages. Antibodies CR8033 and CR8071 recognize distinct conserved epitopes in the head region of the influenza B hemagglutinin (HA), whereas CR9114 binds a conserved epitope in the HA stem and protects against lethal challenge with influenza A and B viruses. These antibodies may inform on development of monoclonal antibody–based treatments and a universal flu vaccine for all influenza A and B viruses.

Influenza viruses continue to cause substantial morbidity and mortality worldwide (*1*). Because current vaccines are typically only effective against the specific viral strains used for vaccination and closely related viruses (*2*) and increasing resistance reduces the effectiveness of the available antiviral drugs (*3*), an urgent need remains for innovative new treatments, both prophylactic and therapeutic (*4*). To this end, we and others have previously described human monoclonal antibodies (mAbs) that neutralize a wide spectrum of influenza A viruses by binding to highly conserved epitopes in the stem region of hemagglutinin (HA), the major viral surface glycoprotein (*5*–*9*). To date, influenza B viruses have received less attention, because they are largely restricted to humans and thus lack the large animal reservoirs that are key to the emergence of pandemic influenza A viruses (*10*).

Although the morbidity and mortality rates attributable to influenza B are lower than those for H3N2 viruses, they are higher than those for H1N1 viruses (*11*). Influenza B viruses are classified as a single influenza type, but two antigenically and genetically distinct lineages cocirculate (*12*), represented by the prototype viruses B/Victoria/2/1987 (Victoria lineage) and B/Yamagata/16/1988 (Yamagata lineage) (*13*). Vaccine manufacturers have therefore recently initiated clinical evaluation of quadrivalent vaccines that include strains from each influenza B lineage, H1N1, and H3N2 (*14*). Given that influenza B viruses are the major cause of seasonal influenza epidemics every 2 to 4 years leading to substantial absenteeism, hospitalization, and death (*11*), mAbs with broad neutralizing activity (bnAbs) against influenza B viruses have important clinical potential.

Combinatorial display libraries, constructed from human B cells of volunteers recently vaccinated with the seasonal influenza vaccine (*9*), were panned by using soluble recombinant HA from various influenza A and B viruses, and phages were subsequently screened for binding to HAs

[1]Department of Molecular Biology, The Scripps Research Institute, 10550 North Torrey Pines Road, La Jolla, CA 92037, USA. [2]Department of Molecular Biology, Gustav Wieds Vej 10C, Aarhus 8000, Denmark. [3]Crucell Vaccine Institute, Janssen Center of Excellence for Immunoprophylaxis, Archimedesweg 4-6, 2301 CA Leiden, Netherlands. [4]State Key Laboratory of Emerging Infectious Diseases and School of Public Health, Li Ka Shing Faculty of Medicine, The University of Hong Kong, 21 Sassoon Road, Pokfulam, Hong Kong, China. [5]Skaggs Institute for Chemical Biology, The Scripps Research Institute, 10550 North Torrey Pines Road, La Jolla, CA 92037, USA.

*These authors contributed equally to this work.
†Present address: Department of Microbiology and Immunology, University of California—San Francisco, 600 16th Street, San Francisco, CA 94143, USA.
‡Present address: Lawrence Berkeley National Laboratory, Department of Bioenergy/GTL and Structural Biology, Berkeley, CA 94720, USA.
§To whom correspondence should be addressed. E-mail: wilson@scripps.edu (I.A.W.); jaap.goudsmit@crucell.com (J.G.)

A

		K_d (nM)		
		CR8033	CR8071	CR9114
Influenza B	B/Lee/1940	3.4	0.9	1.6
Yamagata	B/Nashville/45/1991	0.9	1.2	1.5
Yamagata	B/Harbin/7/1994	0.4	1.1	1.4
Yamagata	B/Houston/B60/1997	0.7	1.0	1.4
Yamagata	B/Jilin/20/2003	0.7	1.0	1.8
Yamagata	B/Florida/4/2006	0.7	0.9	1.3
Yamagata	B/Mississippi/04/2008	1.3	1.1	1.6
Victoria	B/Ohio/01/2005	3.4	1.4	4.8
Victoria	B/Brisbane/60/2008	1.9	1.1	1.5
Victoria	B/Malaysia/2506/2004	18.8	0.9	1.5
Victoria	B/Mississippi/07/2008	3.6	1.3	1.5
Influenza A	A/Puerto Rico/8/1934 H1	>50	>50	0.9
Grp 1	A/New Caledonia/20/1999 H1	>50	>50	1.2
Grp 1	A/Vietnam/1203/2004 H5	>50	>50	0.9
Grp 1	A/Hong Kong/1073/1999 H9	>50	>50	0.6
Grp 2	A/Hong Kong/1/1968 H3	>50	>50	2.2
Grp 2	A/Wisconsin/67/2005 H3	>50	>50	1.9
Grp 2	A/Mal/Netherlands/12/2000 H7	>50	>50	1.1

B

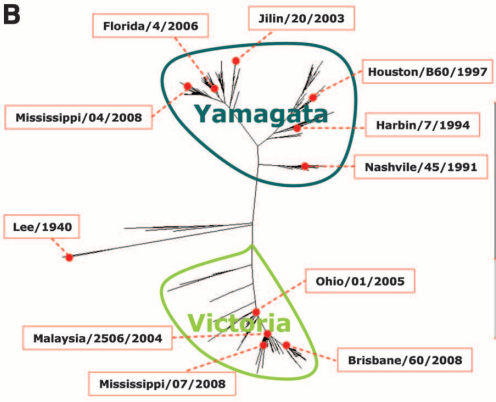

C

		IC_{50} (μg/ml)					
		MN			HI		
		CR8033	CR8071	CR9114	CR8033	CR8071	CR9114
Influenza B	Yamagata: B/Harbin/7/1994	0.03	2.2	>50	0.65	>50	>50
Yamagata	B/Florida/4/2006	0.02	1.7	>50	0.22	>50	>50
Victoria	B/Malaysia/2506/2004	0.9	8.8	>50	>50	>50	>50
Victoria	B/Brisbane/60/2008	5.2	1.6	>50	>50	>50	>50
Influenza A	Grp 1: A/New Caledonia/20/1999 H1	n.a.	n.a.	2.5	n.a.	n.a.	>50
Grp 2	A/Wisconsin/67/2005 H3	n.a.	n.a.	28.6	n.a.	n.a.	>50

Fig. 1. In vitro binding and neutralizing activity of CR8033, CR8071, and CR9114. (**A**) Relative K_d for binding of CR8033, CR8071, and CR9114 to a wide range of influenza A and B HAs as determined by using a fluorescence-based plate assay. The HAs were selected to cover the two lineages and main phylogenetic branches of influenza B, as well as the major subtypes of influenza A that have infected humans. Values are from one representative of three independent experiments and reported in nM. (**B**) Dendrogram of all non-redundant, full-length influenza B HA sequences in the NCBI Flu database (*36*). The positions in the phylogenetic tree of the influenza B HAs used in these studies are indicated. (**C**) Fifty percent inhibitory concentrations (IC_{50}, μg/ml) of CR8033, CR8071, and CR9114 against representative strains from the Yamagata and Victoria lineages of influenza B and the H1N1 and H3N2 subtypes of influenza A as determined by means of microneutralization (MN) and HI assays. Values are representative of three independent experiments and reported in mg/ml. n.a. indicates not applicable.

Fig. 2. In vivo efficacy of CR8033, CR8071, and CR9114. Efficacy of CR8033 (**A**), CR8071 (**B**), and CR9114 (**C**) against lethal challenge with mouse-adapted B/Florida/4/2006 (left) or B/Malaysia/2506/2004 (right) virus and (**D**) of CR9114 against mouse-adapted A/Puerto Rico/8/1934 (left) or A/Hong Kong/1/1968 virus (right). Survival curves of mice [10 animals per group in (A) to (C), 8 per group in (D)] treated with the indicated doses of CR8033, CR8071, or CR9114, or vehicle control 24 hours before challenge by intranasal inoculation (at day 0), are shown. Asterisks indicate significant improvements in survival proportions at day 21 compared with vehicle control ($P < 0.05$).

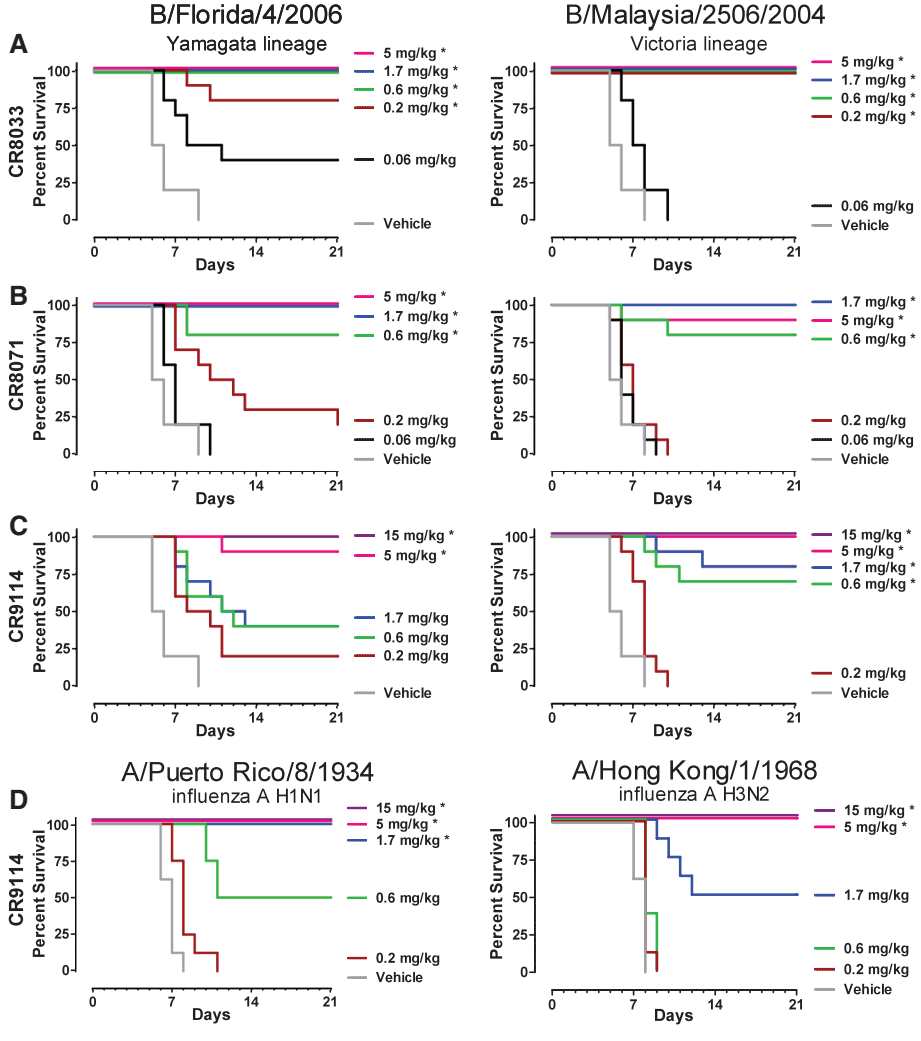

of both influenza B lineages (*15*). We recovered three immunoglobulins (IgGs) that bound HAs from both lineages, CR8033 (V_H3-9 and V_κ3-20) and CR8071 (V_H1-18 and V_λ1-47) (Fig. 1, A and B), as well as CR9114, a V_H1-69 antibody, which additionally binds influenza A viruses from both group 1 and group 2 (Fig. 1A and fig. S1). Importantly, CR8033 and CR8071 neutralized representative viruses from either lineage (Fig. 1C), whereas polyclonal sheep sera did not (table S1). CR8033 showed hemagglutination-inhibition (HI) activity against the Yamagata lineage but not against the Victoria lineage. Thus, whereas CR8033 likely neutralizes Yamagata strains by blocking receptor binding, it appears to neutralize Victoria strains by another mechanism. In contrast, CR8071 showed no HI activity against either lineage. Although CR9114 neutralized all influenza A viruses tested, it did not show in vitro neutralizing activity against influenza B viruses at the tested concentrations (Fig. 1C). Because recent work indicated that the protective efficacy of broadly neutralizing influenza antibody FI6 is substantially dependent on antibody effector functions (*5*), we evaluated the protective efficacy of all three mAbs against B/Florida/4/2006 (Yamagata) and B/Malaysia/2506/2004 (Victoria) infections in mice.

Doses as low as 0.6 mg/kg and 0.2 mg/kg of CR8033 fully protected mice from lethality upon challenge with B/Florida/4/2006 and B/Malaysia/2506/2004, respectively, and lower doses still resulted in increased survival and reduced weight loss (Fig. 2A and fig. S2A). Although CR8071 is somewhat less potent in vivo than CR8033 (Fig. 2B and fig. S2B), the difference is less marked than expected on the basis of the microneutralization assay, indicating that in vitro neutralization is not fully predictive of in vivo potency. Despite the apparent lack of in vitro neutralizing activity, 15 mg/kg and ≥5 mg/kg of CR9114 fully protected mice from lethality after challenge with B/Florida/4/2006 and B/Malaysia/2506/2004, respectively, with significant protection against the latter virus with 1.7 and 0.6 mg/kg (Fig. 2C and fig. S2C). Similarly, 1.7 and 5 mg/kg CR9114 protected mice against challenge with lethal doses of influenza A H1N1 and H3N2 viruses, respectively (Fig. 2D and fig. S2D).

CR8033, CR8071, and CR9114 do not compete with each other for HA binding, suggesting that they recognize different epitopes (fig. S3). However, CR9114 competes with CR6261 and CR8020 (fig. S4), suggesting that it binds an HA stem epitope. To identify their epitopes and understand how they achieve broad neutralization, we obtained x-ray and electron microscopy (EM)

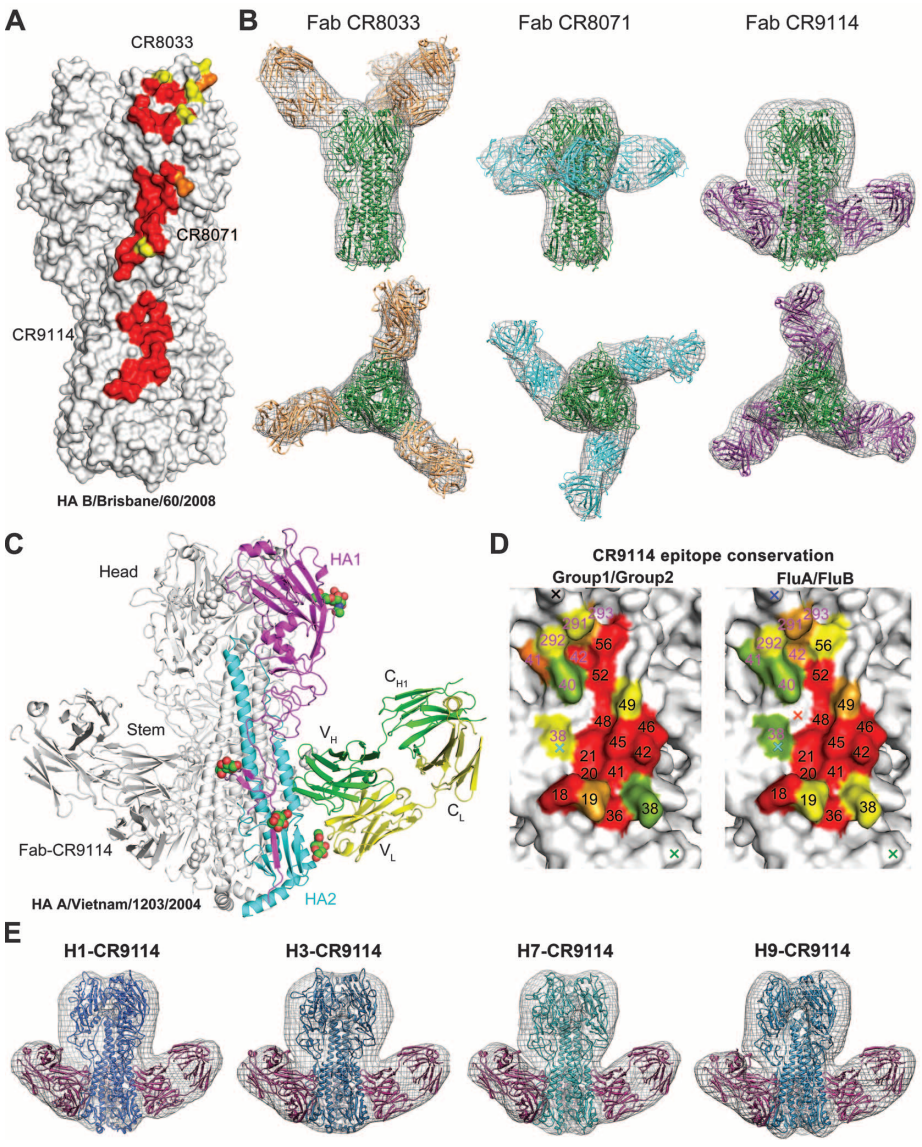

Fig. 3. CR8033, CR8071, and CR9114 bind to distinct epitopes on influenza B HA and conservation of the CR9114 neutralizing epitope on influenza A and B. (**A**) Surface representation illustrating the neutralizing epitopes on HA B/Brisbane/60/2008 of CR8033, CR8071, and CR9114 as determined from the EM structures in (B) and the crystal structures of CR9114 in (C) and CR8071 in fig. S8. The EM density maps allow unambiguous fits of known structures with good correspondence with the CR9114 epitope defined by both x-ray crystallography and EM, despite differences in resolution. The structure is colored by conservation of contact residues across all available influenza B virus sequences: red, over 98% conserved; orange, 75 to 98% conserved; yellow, 50 to 75% conserved. (**B**) Negative stain EM reconstructions (gray mesh) of CR8033 (left), CR8071 (middle), and CR9114 (right) in complex with B/Florida/4/2006. Side (top row) and overhead (bottom row) views show the fits of the individual crystal structures of the Fabs and flu B HA to the EM density. (**C**) Crystal structure of CR9114 in complex with H5 HA (group 1). One HA/Fab protomer of the trimeric complex is colored with HA1 in magenta, HA2 in cyan, Fab heavy chain in green, Fab light chain in yellow, and N-linked glycans in colored balls representing their atom type. The other two protomers are colored in gray. (**D**) Conservation of CR9114 contact residues across all 16 influenza A subtypes (left) and between influenza A and B viruses (right). Red, orange, and yellow correspond to coloring used in (A), with green indicating 25 to 50% conserved. Carbohydrates positions are represented by a cross colored in black (group 1), cyan (group 2), green (group 1 and 2), orange (influenza B), and blue (influenza A and B). Residue numbers are shown with HA1 in magenta and HA2 in black. (**E**) Illustration of cross-reactivity of CR9114 for influenza A (from left to right) H1, H3, H7, and H9 subtypes using negative stain EM. Single-particle reconstructions of negatively stained CR9114 Fabs bound to HA trimers from four major subtypes of influenza A that have infected humans (SC1918/H1, group 1; HK68/H3, group 2; Neth03/H7, group 2; and Wisc66/H9, group 1). The HA trimers are colored in different shades of blue. The Fabs of CR9114 (three per trimer) are colored in purple (the third Fab, at the back, has been omitted for clarity). Broadly neutralizing CR9114 binds in a structurally similar manner to the stem region across all subtypes, groups, and classes of HA. Additional density in the HA not accounted for by the protein likely corresponds to glycosylation.

structures for CR8033, CR8071, and CR9114 (Fig. 3) in complex with representative HAs of influenza A and B viruses.

We generated a 3D reconstruction of the HA ectodomain of B/Florida/4/2006 in complex with Fab CR8033 (Fig. 3B) by using negative stain electron microscopy (EM). Crystal structures of Fab CR8033 at 1.9 Å and influenza B/Brisbane/60/2008 HA ectodomain at 3.45 Å provided atomic models for fitting into the EM reconstruction (fig. S5 and tables S2 to S5). Three CR8033 Fabs bind the HA trimer on an epitope overlapping the receptor-binding pocket and surrounding antigenic sites. The EM model suggests that almost all contacts are made by variable region of heavy chain (V_H) using all three heavy-chain complementarity-determining region (HCDRs) loops and framework 3 (fig. S6) (*16*). Although the receptor-binding pocket of influenza B HA is well conserved, variability in surrounding residues (fig. S7) may account for differences in CR8033 binding and neutralization of the two influenza B lineages.

EM reconstructions were also performed on Fab CR8071 in complex with both B/Florida/4/2006 (Yamagata) and B/Malaysia/2506/2004 HAs (Victoria) (Fig. 3B and fig. S8D), along with crystal structures of Fab CR8071 with a B/Florida/4/2006 HA1 construct (2.7 Å) and CR8059, of which CR8071 is a stabilized variant (see supplementary materials), with B/Brisbane/60/2008 HA (5.65 Å) (fig. S8, A to C). CR8071 binds the vestigial esterase domain at the base of the HA head distant from the receptor-binding site and in an orientation (Fig. 3B) consistent with the observed lack of HI. The epitope is highly conserved in influenza B HA, with 17 of 19 residues >98% conserved.

Crystal structures were determined for Fab CR9114 with HAs from a highly pathogenic H5N1 virus (A/Vietnam/1203/2004; Viet04/H5, 1.7 Å) (Fig. 3C), as well as H3 (5.25 Å) and H7 (5.75 Å) (fig. S9). EM studies further illustrated the CR9114 cross-reactivity with influenza A H1, H3, H7, and H9 subtypes and influenza B (Fig. 3E). CR9114 binds the HA stem (fig. S10), recognizing an epitope nearly identical to that of CR6261 (*17*) by using the same HCDR loops (1, 2, 3) and FR3 with no light-chain contacts. Recently, human antibody FI6 was identified that broadly neutralizes influenza A viruses by targeting about the same epitope (*5*). However, FI6 uses a different V gene (V_H3-30) and its light chain (fig. S11) and is rotated by ~90° compared with V_H1-69 antibodies CR6261 and CR9114. Thus, FI6 represents an alternative solution to cross-group neutralization of influenza A but not influenza B viruses.

The CR9114 epitope is highly conserved in essentially all influenza A subtypes and influenza B (Fig. 3D and tables S6 and S7). At least three obstacles must be overcome for an antibody to bind to a similar epitope across influenza A and B. First, most group 1 HAs have HA2 Thr^{49}, whereas most group 2 HAs have a larger Asn (fig. S10 and table S6) (*6*, *18*) that can be accommodated by CR9114. Second, polymorphisms at HA2 position 111, His (group 1), Thr/Ala (group 2), or Glu (influenza B), result in subtly different conformations of HA2 Trp^{21}, which affect its ability to make favorable interactions with hot spot residue HCDR2 Phe^{54} in CR6261 (fig. S10) (*19*). The more favorable orientation and approach of Phe^{54} and the apparent plasticity of the CR9114 combining site (*20*) (fig. S12) may allow CR9114 to make high-affinity interactions (including a hydrogen bond) with the various conformations of Trp^{21} in group 1 and group 2 HAs. Third, the predominant conformation of a conserved glycan at HA1 Asn^{38} in H3, H7, H10, and H15 in group 2,

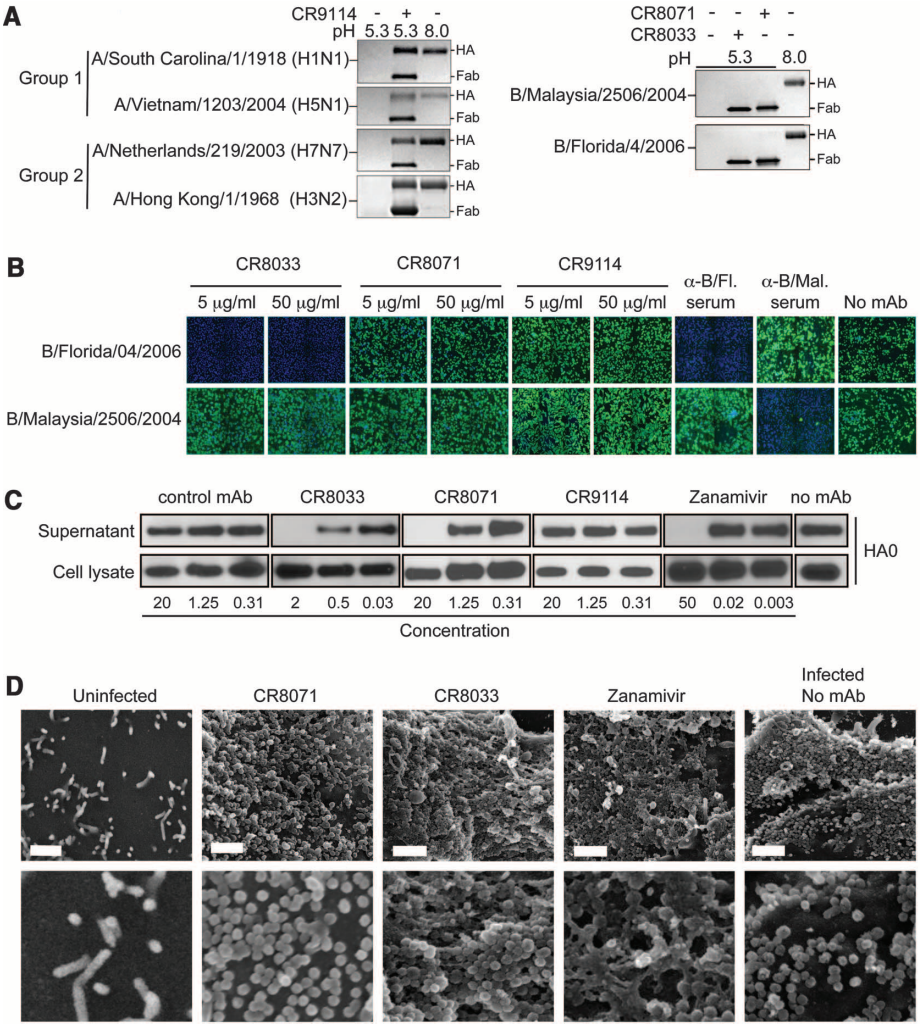

Fig. 4. Neutralization mechanisms of CR8033, CR8071, and CR9114. (**A**) CR9114 protects HAs of group 1 [A/South Carolina/1/1918 (H1N1) and A/Vietnam/1203/2004 (H5N1)] and group 2 [A/Netherlands/219/2003 (H7N7) and A/Hong Kong/1/1968 (H3N2)] influenza A viruses from the pH-induced protease sensitivity associated with membrane fusion. Exposure to low pH converts the HAs to the postfusion state, rendering them sensitive to trypsin digestion (lane 1 versus 3), but CR9114 prevents this conversion, retaining the HA in the protease-resistant, prefusion form (lane 2). CR8033 and CR8070 do not prevent this conversion at low pH (right) ($N = 4$). (**B**) Expression of influenza NP in monolayers of MDCK cells 16 to 18 hours after inoculation with B/Florida/4/2006 or B/Malaysia/2506/2004 viruses that were preincubated with CR8033, CR8071, CR9114, or polyclonal sheep sera directed against B/Florida/4/2006 or B/Malaysia/2506/2004, as indicated. NP expression is determined by immunofluorescence. Representative images of three independent experiments are shown. (**C**) Immunoblots of uncleaved HA (HA0) detected in the lysate and supernatant of MDCK cells infected with B/Florida/4/2006 virus and subsequently (from 3 to 20 hours postinfection) incubated with different concentrations of antibodies or zanamivir as indicated. HA0 was detected by using rabbit serum against B/Jiangsu/10/03 (Yamagata lineage). Concentrations are in μg/ml and μM for antibodies and zanamivir, respectively. Results from one representative of two independent experiments are shown. (**D**) SEM images of the surface of MDCK cells infected with B/Florida/4/2006 virus and subsequently (from 3 to 20 hours postinfection) incubated with CR8071 (10 μg/ml), CR8033 (2.5 μg/ml), or zanamivir (60 μM). Representative images of three independent experiments are shown. Scale bar, 1 μm.

and at HA1 Asn^{332} in influenza B, would obscure the epitope surface (figs. S10 and S11) (*21*–*23*). Thus, this glycan and Asn side chain must be able to adopt a permissive alternative conformation as observed in the CR9114-H3 crystal structure (*24*). Displacement of the HA1 38 glycan appears essential for CR9114 binding to several influenza A subtypes, and a similarly positioned glycan at HA1 332 in influenza B must also be avoided (fig. S11). Such glycan flexibility at HA1 38 was also observed in the FI6 structure with H3 HA, but, in this case, the glycan at 332 in flu B may be more difficult to avoid (*25*).

CR9114 and CR6261 both use the V_H1-69 germline V gene and have relatively small numbers of somatic mutations compared with other bnAbs (*26*, *27*). However, only five mutations are shared (fig. S13), and, hence, they are not simple variants of one another. Aside from the heavy-chain–only binding, both antibodies are fairly conventional, in contrast to many bnAbs to other viruses, such as HIV-1, that have unusual features, such as extensive hypermutation, long indels in one or more CDRs, tyrosine sulfation, or domain swapping (*26*, *27*). Consequently, antibodies like CR9114 are likely to be readily generated and may be present in the repertoire of many individuals, suggesting that an appropriate vaccination strategy may be able to selectively amplify such cross-reactive clones and trigger a bnAb response (*4*, *28*, *29*).

Despite CR8033 and CR8071 binding to the more variable HA globular head but consistent with the apparent high level of epitope conservation, escape variants could only be generated after extensive passaging. For B/Florida/4/2006 virus, no CR8033 escape variants were generated in 20 passages, whereas 15 passages were required to generate Lys^{38}→Glu^{38} (Lys38Glu) and Tyr40His mutants with reduced CR8071 susceptibility. For B/Malaysia/2506/2004 virus, 15 passages were required to generate a Pro161Gln reduced susceptibility mutant for CR8033, whereas 20 rounds of passaging did not result in any CR8071 escape variants. Lys^{38} and Pro^{161} are highly conserved (99.4% and 100%, respectively) in all 494 (unique) full-length influenza B HA sequences in the National Center for Biotechnology Information (NCBI) database. Although Tyr^{40} is only 29.1% conserved, all other strains have His^{40}, including B/Harbin/7/94, B/Malaysia/2506/04, and B/Brisbane/60/08, which are effectively neutralized by CR8071 (Fig. 1C). In contrast, the Lys38Glu mutation has not been observed in any influenza B isolates. Because CR9114 does not neutralize influenza B viruses in vitro, no influenza B escape variants could be generated (*30*).

The identification of conserved neutralizing epitopes in the influenza B HA globular head parallels the recent identification of such epitopes in influenza A viruses (*31*, *32*) and establishes that both the HA stem and head regions contain broadly protective epitopes. Whereas the stem-binding CR9114 blocks the HA pH-induced conformational changes associated with membrane fusion (Fig. 4, A and B, and figs. S14 and S15) (*33*), this mechanism is not applicable to CR8033 and CR8071 that bind the head region (Fig. 4A). Indeed, whereas CR8033 has HI activity and blocks viral infection when preincubated with B/Florida/4/2006 virus, it had no such effect on B/Malaysia/2506/2004 virus (Fig. 1C and Fig. 4B). Furthermore, CR8071 did not prevent infection of cells by either virus (Fig. 4B) (*34*).

These antibodies appear to prevent propagation of viruses without preventing entry and genome replication (Figs. 1C and 4B). Thus, we assessed the effect of CR8033 and CR8071 on formation of viral progeny from infected cells. Whereas HA was readily detected in both lysates and supernatants of Madin-Darby canine kidney (MDCK) cell cultures that were first infected and subsequently incubated with a nonbinding control antibody or CR9114, no HA could be detected in the supernatants upon incubation with CR8033 or CR8071, despite abundant HA in the lysate (Fig. 4C). The effects of CR8033 and CR8071 then resemble that of neuraminidase inhibitor zanamivir, which interferes with release of progeny virions from infected cells (*35*). Indeed, the dense aggregation of virions on the surface of infected cells, particularly in the presence of antibody CR8033, closely resembles that observed in zanamivir-treated cells as examined by scanning electron microscopy (SEM) (Fig. 4D).

The identification and characterization of monoclonal antibodies with broad neutralizing activity against influenza B viruses, together with previously described broadly neutralizing antibodies against group 1 and group 2 influenza A viruses (*6*, *7*, *9*), bring a universal therapy a step closer and may serve as guides for design of broadly protective vaccines. In particular, a vaccine that elicits antibodies targeting the CR9114 epitope may provide the ultimate goal of protection against all influenza A and influenza B viruses.

References and Notes

1. World Health Organization (WHO), Fact sheet 211: Influenza (2009); www.who.int/mediacentre/factsheets/2003/fs211/en/.
2. S. Salzberg, *Nature* **454**, 160 (2008).
3. A. C. Lowen, P. Palese, *Infect. Disord. Drug Targets* **7**, 318 (2007).
4. T. T. Wang, P. Palese, *Nat. Struct. Mol. Biol.* **16**, 233 (2009).
5. D. Corti *et al.*, *Science* **333**, 850 (2011); 10.1126/science.1205669.
6. D. C. Ekiert *et al.*, *Science* **324**, 246 (2009); 10.1126/science.1171491.
7. D. C. Ekiert *et al.*, *Science* **333**, 843 (2011); 10.1126/science.1204839.
8. J. Sui *et al.*, *Nat. Struct. Mol. Biol.* **16**, 265 (2009).
9. M. Throsby *et al.*, *PLoS One* **3**, e3942 (2008).
10. A. D. Osterhaus, G. F. Rimmelzwaan, B. E. Martina, T. M. Bestebroer, R. A. Fouchier, *Science* **288**, 1051 (2000).
11. W. W. Thompson *et al.*, *JAMA* **292**, 1333 (2004).
12. M. Yamashita, M. Krystal, W. M. Fitch, P. Palese, *Virology* **163**, 112 (1988).
13. P. A. Rota *et al.*, *Virology* **175**, 59 (1990).
14. C. S. Ambrose, M. J. Levin, *Hum. Vaccin. Immunother.* **8**, 81 (2012).
15. Materials and methods are available as supplementary materials on *Science* Online.
16. We have previously shown (our previous control analyses of CR6261 and other known HA-Fab complexes) that, because we have high-resolution crystal structures of HAs and antibodies, the fit to the density is excellent and generally unambiguous. Nevertheless, the lower resolution of these data does not permit as precise a definition of the Ab epitope.
17. This epitope consists of residues from the N- and C-terminal regions of HA1 (38, 40 to 42, and 291 to 293), and the N-terminal portion of HA2 (18 to 21, 36, 38, 41, 42, 45, 46, 48, 49, 52, 53, and 56), including helix A. CR9114 buries a total of ~1293 $Å^2$ at the interface with HA (654 $Å^2$ for HA and 639 $Å^2$ for Fab).
18. Thr^{49} is buried by CR6261, and affinity of CR6261 for the SC1918/H1 HA is reduced over 100-fold by a Thr49Asn mutation designed to mimic the group 2 sequence. Further, CR6261 binding to H12 HA (group 1) is undetectable under our assay conditions [binding affinity (K_d) > ~10 μM], likely because of a Thr49Gln substitution. In contrast, CR9114 binds the SC1918/H1 Thr49Asn mutant and H12 HA (Thr49Gln) with high affinity because the conformation of its HCDR1 loop allows the larger Asn and Gln side chains to be accommodated.
19. A His111Leu mutation that mimics the group 2 Trp^{21} conformation on a group 1 background drastically reduces CR6261 binding and correlates with virus escape from neutralization (*9*).
20. HCDRs 1, 2, and 3 adopt substantially different conformations in the unbound CR9114 and the CR9114-H5 complex crystal structures, suggesting that these loops may be quite flexible in solution (fig. S12) and allow the antibody to adapt to the subtle variation seen in the largely conserved epitope in HA proteins from different virus subtypes and types.
21. Y. Ha, D. J. Stevens, J. J. Skehel, D. C. Wiley, *Virology* **309**, 209 (2003).
22. Q. Wang, F. Cheng, M. Lu, X. Tian, J. Ma, *J. Virol.* **82**, 3011 (2008).
23. H. Yang, L. M. Chen, P. J. Carney, R. O. Donis, J. Stevens, *PLoS Pathog.* **6**, e1001081 (2010).
24. This alternate glycan configuration is supported by the observation of additional electron density near Asn^{38} in the CR8020-H3 crystal structure, indicating at least two accessible glycan conformations (*7*). Although not modeled explicitly, the second conformation would move the glycan away from the epitope and facilitate antibody binding.
25. Although isolate-specific variation in residues proximal to the epitope may also influence interaction of FI6 with influenza B, one possible problem is the Tyr100C at the tip of HCDR3 that makes an H bond with Thr^{318} (group1/2) in the hydrophobic groove at the junction between helix A and HA1 (fig. S10). In influenza B, the equivalent residue is a glycosylated Asn^{332}, which will likely lead to a steric clash with Tyr100C of FI6. CR9114 does not interact with Thr^{318}, and the orientation of the HCDR2 loop allows CR9114 to accommodate larger residue at this position (figs. S10 and S11).
26. L. M. Walker *et al.*, *Science* **326**, 285 (2009); 10.1126/science.1178746.
27. T. Zhou *et al.*, *Science* **329**, 811 (2010); 10.1126/science.1192819.
28. C. J. Wei *et al.*, *Science* **329**, 1060 (2010); 10.1126/science.1192517.
29. J. Wrammert *et al.*, *J. Exp. Med.* **208**, 181 (2011).
30. No escape variants were generated; however, two substitutions previously described to affect neutralization of group 2 and group 1 influenza A viruses by CR8020 and CR6261, respectively, also affected CR9114 binding. Asp19Asn affects H3 and H7 viruses and reduces H3 binding (~30-fold increase in K_d). In addition, all influenza B viruses have Ala^{19}, which may account in part for the somewhat lower affinity for influenza B. In contrast, several group 1 subtypes with Asp19Asn or Asp19Ala mutations are neutralized by CR9114 and/or bound with high affinity, presumably because other substitutions offset the detrimental effect of substitutions at position 19. The Asp19Asn variant is rare in most subtypes, suggesting that most viruses will be sensitive

to CR9114 (table S7) (*7*). The other Ile45Phe escape variant is naturally present in essentially all human H2N2 viruses that circulated from 1957 to 1968, and Phe45Ile substitution in a human H2 HA restores high affinity binding for both CR6261 and CR9114 (table S8). In contrast, Phe^{45} occurs in only 3 of 8550 sequences from avian H2N2 isolates and the remaining 15 subtypes.
31. J. C. Krause *et al*., *J. Virol.* **85**, 10905 (2011).
32. J. R. Whittle *et al*., *Proc. Natl. Acad. Sci. U.S.A.* **108**, 14216 (2011).
33. Why influenza B viruses are not neutralized in the same way by CR9114 remains currently unknown.
34. In contrast, polyclonal sheep sera directed against B/Florida/4/2006 and B/Malaysia/2506/2004 did prevent initial infection, but not of virus from the opposite lineage.
35. L. V. Gubareva, L. Kaiser, F. G. Hayden, *Lancet* **355**, 827 (2000).
36. Y. Bao *et al*., *J. Virol.* **82**, 596 (2008).

Acknowledgments: We thank J. Juraszek; B. Brandenburg; M. Koldijk; K. Hegmans; J. Meijer; N. Hafkemeier; A. Apetri; J. Dulos; L. Dekking; H. Vietsch; G. Perdok; H. Tien; D. Marciano; the staff of the Advanced Photon Source (APS) GM/CA-CAT 23ID-B and 23ID-D, Stanford Synchrotron Radiation Lightsource (SSRL) BL11-1 and SSRL BL7-1, and Advanced Light Source (ALS); X. Dai; R. Stanfield; W. Yu; J. P. Julien; R. N. Kirchdoerfer; and E. Brown of Ottawa University, Canada, for the mouse-adapted A/Hong Kong/1/68 strain. Crystallization experiments were carried out on the Rigaku Crystalmation system at the Joint Center for Structural Genomics, which is supported by the National Institute of General Medical Sciences (NIGMS) Protein Structure Initiative U54 GM094586. The EM and image analysis was conducted by R.K., J.H.L., and Z.M. at the National Resource for Automated Molecular Microscopy, which is supported by NIH through the National Center for Research Resources' P41 program (RR017573). This project has been funded in part by the Area of Excellence Scheme of the University Grants Committee, Hong Kong (grant AoE/M-12/06); a predoctoral fellowship from the Achievement Rewards for College Scientists Foundation (D.C.E.); grant GM080209 from the NIH Molecular Evolution Training Program (D.C.E.); a Saper Aude Postdoc grant from the Danish Council for Independent Research, Natural Sciences (N.S.L.), and the Skaggs Institute (I.A.W.). Portions of this research were carried out at the SSRL, a national user facility operated by Stanford University on behalf of the U.S. Department of Energy (DOE), Office of Basic Energy Sciences. The SSRL Structural Molecular Biology Program is supported by the DOE Office of Biological and Environmental Research and by NIH, National Center for Research Resources, Biomedical Technology Program (P41RR001209), and the NIGMS. The GM/CA CAT 23-ID-B beamline has been funded in whole or in part with federal funds from National Cancer Institute (Y1-CO-1020) and NIGMS (Y1-GM-1104). Use of the APS was supported by the DOE, Basic Energy Sciences, Office of Science, under contract no. DE-AC02-06CH11357. The content is solely the responsibility of the authors and does not necessarily represent the official views of NIGMS or the NIH. The ALS is supported by the director, Office of Science, Office of Basic Energy Sciences, of the DOE under contract no. DE-AC02-05CH11231. Coordinates and structure factors are deposited in the Protein Data Bank (PDB code 4FQH for CR9114 Fab, 4FQI for CR9114 Fab-A/H5 HA, 4FQJ for CR8071 Fab-B/Florida HA1, 4FQK for CR8059 Fab-B/Brisbane HA, 4FQL for CR8033 Fab, 4FQM for B/Brisbane HA, 4FQY for CR9114 Fab-A/H3 HA, and 4FQV for CR9114 Fab-A/H7 HA). Image reconstructions have been deposited at the EMDataBank under accession numbers EMD-2143 (CR8033/Florida), EMD-2144 (CR8071/Florida), EMD-2145 (CR8071/Malaysia), EMD-2146 (CR9114/Florida), EMD-2147 (CR9114/H1), EMD-2148 (CR9114/H3), EMD-2149 (CR9114/H9), and EMD-2150 (CR9114/H7). Nucleotide sequences for the CR8033, CR8059 (CR8071), and CR9114 variable regions have been deposited in GenBank [accession numbers JX213635 (CR8033, V_H), JX213636 (CR8033, V_κ), JX213637 (CR8059, V_H), JX213638 (CR8059, V_λ), JX213639 (CR9114, V_H), and JX213640 (CR9114, V_λ)]. Patent applications relating to antibodies CR8033, CR8059, CR8071, and CR9114 have been filed (CR8033, CR8059, and CR8071 are claimed in EP 12158525.1 and U.S. 61/608,414. CR9114 is claimed in EP 11173953.8 and U.S. 61/572,417). Sharing will be subject to standard material transfer agreements. This is publication 21741 from the Scripps Research Institute.

Supplementary Materials
www.sciencemag.org/cgi/content/full/science.1222908/DC1
Materials and Methods
Figs. S1 to S18
Tables S1 to S8
References (*37*–*62*)

4 April 2012; accepted 9 July 2012
Published online 9 August 2012;
10.1126/science.1222908

Structural Probing of a Protein Phosphatase 2A Network by Chemical Cross-Linking and Mass Spectrometry

Franz Herzog,[1]* Abdullah Kahraman,[1]* Daniel Boehringer,[2]* Raymond Mak,[1] Andreas Bracher,[4] Thomas Walzthoeni,[1] Alexander Leitner,[1] Martin Beck,[3] Franz-Ulrich Hartl,[4] Nenad Ban,[2] Lars Malmström,[1] Ruedi Aebersold[1]†

The identification of proximate amino acids by chemical cross-linking and mass spectrometry (XL-MS) facilitates the structural analysis of homogeneous protein complexes. We gained distance restraints on a modular interaction network of protein complexes affinity-purified from human cells by applying an adapted XL-MS protocol. Systematic analysis of human protein phosphatase 2A (PP2A) complexes identified 176 interprotein and 570 intraprotein cross-links that link specific trimeric PP2A complexes to a multitude of adaptor proteins that control their cellular functions. Spatial restraints guided molecular modeling of the binding interface between immunoglobulin binding protein 1 (IGBP1) and PP2A and revealed the topology of TCP1 ring complex (TRiC) chaperonin interacting with the PP2A regulatory subunit 2ABG. This study establishes XL-MS as an integral part of hybrid structural biology approaches for the analysis of endogenous protein complexes.

Cellular processes can rarely be attributed to the activity of a single protein. Instead, proteins act in functional modules, such as macromolecular complexes or signal transduction networks. Gaining mechanistic insights into the function of multisubunit modules is facilitated by structural elucidation (*1*, *2*). Chemical cross-linking, in combination with mass spectrometry (XL-MS), is a low-resolution structural technique for the characterization of the architecture of protein complexes (*3*, *4*). XL-MS provides distance information by identifying spatially proximate lysine residues that have been covalently linked by a bifunctional cross-linking reagent. This approach has been successfully applied to homogenous protein complexes purified for crystallographic purposes (*5*–*8*). In contrast to high-resolution structural biology techniques, XL-MS has the potential to acquire spatial restraints from heterogeneous protein samples. We thus applied this method to characterize the topology of a signaling network by systematic analysis of endogenous protein complexes (Fig. 1).

The abundant protein phosphatase 2A (PP2A) is involved in diverse signaling pathways regulating cell growth, apoptosis, differentiation, cell motility, DNA damage response, and cell cycle progression (*9*–*12*). In eukaryotes, active PP2A holoenzymes are heterotrimers composed of a catalytic subunit (C, human isoforms PP2AA and PP2AB), a scaffold subunit (A, human isoforms 2AAA and 2AAB), and one of a large array of regulatory subunits (B, B', B", and B"', each subfamily consisting of two to five isoforms) (Fig. 2A and table S1) that selectively target PP2A subpopulations to specific substrates (*13*). To reveal the topology of PP2A holoenzymes in complex with the adaptor proteins that regulate their phosphatase activity and subcellular location, we purified these complexes from human cells and analyzed their topology by combining XL-MS and computational molecular modeling.

We first determined the proteins copurifying with trimeric PP2A holoenzymes by isolating 14 proteins, previously detected in PP2A complexes (*14*, *15*), through an N-terminal His_6-HA-StrepII-tag from human embryonic kidney cells (fig. S1 and table S2). The associated protein complexes were identified by mass spectrometry (Fig. 1) (*16*), resulting in a dense interaction network of 94 proteins (Fig. 2A and tables S1 and S3).

To elucidate the topology of the PP2A network, we probed the complexes by XL-MS. Cross-linking was achieved by immobilizing the PP2A complexes on beads (*16*). Incubation with the appropriate concentration of disuccinimidyl suberate (DSS) (fig. S2) and subsequent proteolysis resulted in a complex mixture of tryptic peptides that was

[1]Department of Biology, Institute of Molecular Systems Biology, Eidgenössische Technische Hochschule Zürich, Wolfgang-Pauli Strasse 16, 8093 Zurich, Switzerland. [2]Department of Biology, Institute of Molecular Biology and Biophysics, Eidgenössische Technische Hochschule Zürich, Schafmattstrasse 20, 8093 Zurich, Switzerland. [3]European Molecular Biology Laboratory, Meyerhofstraße 1, 69117 Heidelberg, Germany. [4]Department of Cellular Biochemistry, Max Planck Institute of Biochemistry, Am Klopferspitz 18, 82152 Martinsried, Germany.

*These authors contributed equally to this work.
†To whom correspondence should be addressed. E-mail: aebersold@imsb.biol.ethz.ch